AD-A089 132 DAVID W TAYLOR NAVAL SHIP RESEARCH AND DEVELOPMENT CE--ETC F/G 11/9
MODELING OF INELASTIC BEHAVIOR OF STRUCTURES USING PLASTIC AND --ETC(U)
AUG 80 R A SWANEK, J L RODD, H M FORD
UNCLASSIFIED DTNSRDC-80/073 NL

1 OF 1
AD
A089132

END
DATE
FILMED
10-80
DTIC

AD A089132

UNCLASSIFIED

SECURITY CLASSIFICATION OF THIS PAGE (When Data Entered)

REPORT DOCUMENTATION PAGE

READ INSTRUCTIONS BEFORE COMPLETING FORM

1. REPORT NUMBER: DTNSRDC-80/073 (14)

2. GOVT ACCESSION NO.: AD-A089 132

3. RECIPIENT'S CATALOG NUMBER

4. TITLE (and Subtitle) (6): MODELING OF INELASTIC BEHAVIOR OF STRUCTURES USING PLASTIC AND METAL LAMINATES

5. TYPE OF REPORT & PERIOD COVERED (9): Final rept.

6. PERFORMING ORG. REPORT NUMBER

7. AUTHOR(s) (10): Richard A. Swanek, James L. Rodd, Harry M. Ford and Alfred L. Dinsenbacher

8. CONTRACT OR GRANT NUMBER(s)

9. PERFORMING ORGANIZATION NAME AND ADDRESS: David W. Taylor Naval Ship Research and Development Center, Bethesda, Maryland 20084

10. PROGRAM ELEMENT, PROJECT, TASK AREA & WORK UNIT NUMBERS: (See reverse side)

11. CONTROLLING OFFICE NAME AND ADDRESS

12. REPORT DATE (11): August 1980

13. NUMBER OF PAGES: 53

14. MONITORING AGENCY NAME & ADDRESS (if different from Controlling Office) (12) 53

15. SECURITY CLASS. (of this report): UNCLASSIFIED

15a. DECLASSIFICATION/DOWNGRADING SCHEDULE

16. DISTRIBUTION STATEMENT (of this Report) (16) 2R023 03 (17) 2R023 03 01

APPROVED FOR PUBLIC RELEASE: DISTRIBUTION UNLIMITED

17. DISTRIBUTION STATEMENT (of the abstract entered in Block 20, if different from Report)

18. SUPPLEMENTARY NOTES

19. KEY WORDS (Continue on reverse side if necessary and identify by block number)

Modeling
Inelastic Modeling
Ultimate Strength
Composite Material Models
Structural Modeling

20. ABSTRACT (Continue on reverse side if necessary and identify by block number)

A review of past research concerning the determination of structural ultimate strength and/or inelastic behavior in isotropic metallic structures revealed that (1) most investigations of this type are carried out on full-size or nearly full-size models requiring large test loads and facilities, (2) small-scale modeling of this structural behavior using the parent metal requires a high degree of skill in the fabrication of the model and a subsequent high cost, and (3) no useful and cost effective method of extending

(Continued on reverse side)

DD FORM 1 JAN 73 1473 EDITION OF 1 NOV 65 IS OBSOLETE

S/N 0102-LF-014-6601

UNCLASSIFIED

SECURITY CLASSIFICATION OF THIS PAGE (When Data Entered)

387682

(Block 10)

Program Element 61162N
IRED Program
Task Area ZR0230301
Work Unit 1730-348

(Block 20 continued)

small-scale structural modeling into the inelastic range currently exists. The basic criteria to be satisfied when modeling an isotropic metallic structure elastoplastically using another material are: duplication of stress/modulus versus strain behavior for both model and prototype materials and equality of Poisson's ratio for model and prototype material. Additionally, a structural model using another material must possess the same bending, axial, torsional, and buckling properties as the prototype structure using the parent material. A composite material made up of stainless steel and rigid vinyl was developed to model a mild steel parent material. This composite material was then shown to satisfy the basic criteria needed to elastoplastically model a structure through tests which defined the elastic and inelastic material properties in tension and bending. A deep plate girder structure, for which ultimate strength data exists, was modeled using the composite material and tested. Both the failure mode and ultimate strength of the mild steel girder were accurately reproduced using the composite material. The engineering analyses conducted and their verification through the testing program demonstrate the potential benefits of the composite approach for elastoplastic modeling.

Accession For
NTIS GRA&I
DDC TAB
Unannounced
Justification
By
Distribution/
Availability Codes
Dist | Avail and/or special
A

TABLE OF CONTENTS

	Page
LIST OF FIGURES	iv
LIST OF TABLES	v
ABSTRACT	1
ADMINISTRATIVE INFORMATION	1
METRIC CONVERSION	2
INTRODUCTION	2
BACKGROUND	3
PHOTOELASTIC MATERIALS	4
METAL-FILLED EPOXIES	5
RIGID VINYL	6
FIBERGLASS-TYPE MATERIALS	7
LITERATURE SEARCH SUMMARY	7
BASIC CRITERIA FOR ELASTOPLASTIC MODELING	7
THEORY FOR COMPOSITE MATERIAL	9
EXPERIMENTAL VALIDATION	22
COMPOSITE MATERIALS	24
FABRICATION OF COMPOSITE PLATES	24
TENSION TESTS	26
BENDING TESTS	29
BUCKLING TESTS	33
PLATE GIRDER ULTIMATE STRENGTH TESTS	34
SUMMARY AND CONCLUSIONS	41
ACKNOWLEDGMENTS	43
REFERENCES	45

LIST OF FIGURES

Page

1 - Comparison of Model and Prototype Materials 5

2 - Concentrated and Uniformly Distributed Reinforcement Concepts and Load-Strain Behavior 11

3 - Design Curves for Selecting Percent Area of Reinforcement Needed 13

4 - Uniform and Concentrated Reinforcement Sections and Stress Distributions Across Cross Sections for Elastic and Plastic Cases 15

5 - Comparison of Reinforcement Location on Bending Behavior 17

6 - Critical Buckling Stress versus Slenderness Ratio for a Composite Material 20

7 - Stress-Strain Characteristics of Steel Reinforcement 27

8 - Stress-Strain Characteristics of 30-5-15 Composite 28

9 - Stress-Strain Characteristics of 60-5-25 Composite 30

10 - Bending Specimen Test Setup and Typical Specimen 31

11 - 30-5-15 Composite Layup Bending Moment versus Outer Fiber Strain Characteristics 32

12 - 60-5-25 Composite Layup Bending Moment versus Outer Fiber Strain Characteristics 34

13 - Sketch of Composite Girder Configuration 35

14 - Web Crippling Failure of Composite Girder 1 37

15 - Web Buckling of Composite Girder 2 38

16 - Load versus Midspan Deflection for Girder 2 39

17 - Diagonal Tension Strain Patterns and Growth of Membrane Strain with Load 40

LIST OF TABLES

Page

1 - Comparison of Commonly Employed Modeling Materials 8

2 - Typical Scaling Relationships for Elastic-Plastic Modeling 23

3 - Experimental and Calculated Material Properties for Steel-Reinforced Rigid Vinyl Composite 29

ABSTRACT

A review of past research concerning the determination of structural ultimate strength and/or inelastic behavior in isotropic metallic structures revealed that (1) most investigations of this type are carried out on full-size or nearly full-size models requiring large test loads and facilities, (2) small-scale modeling of this structural behavior using the parent metal requires a high degree of skill in the fabrication of the model and a subsequent high cost, and (3) no useful and cost effective method of extending small-scale structural modeling into the inelastic range currently exists. The basic criteria to be satisfied when modeling an isotropic metallic structure elastoplastically using another material are: duplication of stress/modulus versus strain behavior for both model and prototype materials and equality of Poisson's ratio for model and prototype material. Additionally, a structural model using another material must possess the same bending, axial, torsional, and buckling properties as the prototype structure using the parent material. A composite material made up of stainless steel and rigid vinyl was developed to model a mild steel parent material. This composite material was then shown to satisfy the basic criteria needed to elastoplastically model a structure through tests which defined the elastic and inelastic material properties in tension and bending. A deep plate girder structure, for which ultimate strength data exists, was modeled using the composite material and tested. Both the failure mode and ultimate strength of the mild steel girder were accurately reproduced using the composite material. The engineering analyses conducted and their verification through the testing program demonstrate the potential benefits of the composite approach for elastoplastic modeling.

ADMINISTRATIVE INFORMATION

The results presented in this report were sponsored by the Independent Research and Exploratory Development Program, Task Area ZR0230301 of Program Element 61152N under Work Unit 1730-348. The work was performed in the Surface Ship Division of the Structures Department of the David W. Taylor Naval Ship Research and Development Center (DTNSRDC).

METRIC CONVERSION

1 inch (in.) = 2.54 centimeters

1 pound (lb) = 4.448 newtons

1 gallon (gal) = 3.8 liters

1 pound per square inch (psi) = 6.895×10^3 pascals

1 kip (1000 pounds force) = 4.448×10^3 newtons

1 kip per square inch (ksi) = 6.895×10^6 pascals

1 inch pound (in. lb) = 0.113 newton meters

INTRODUCTION

The problem of determining the ultimate strength of a structure wherein various components experience inelastic strains, buckling and post buckling has been the subject of much research by the engineering community. High performance naval ships or naval and merchant ships of a more standard design are subjected to loads which can, statistically, result in severe local damage or overall structural failure. Much work has been done in the area of structural ultimate strength, primarily in the civil engineering community. Some theoretical work has been performed, but most research has centered upon the results of model and full-scale tests to develop methods by which structural ultimate strength can be predicted (References 1 through 5, for example).* It is not unusual to find that a large- or full-size model was constructed to obtain experimental data, usually at great expense. These models are generally made of the same material as the prototype, thus assuring similarity for a number of engineering parameters. A number of problems arise with modeling small-scale metallic ship structures. The first problem is one of fabrication. While it is not difficult to join large sheets of steel, fastening smaller, thinner sheets requires greater skill and attention to detail. For instance, it may be impractical to weld very thin plates, especially when one tries to weld in limited access places in a scaled-down model. The control of burnthrough, welding distortions, and residual stresses requires the use of highly skilled labor and leads to higher fabrication costs. Problems may also arise in testing due to the local loading of thin plates required for accurate scaling or primary loads. Additionally, scale-thickness sizes of the metal may not be available. Most models would also require

*A complete listing of references is given on page 45.

large loads to attain the correctly modeled prototype loads. This could involve an extensive, expensive test setup and facility. Furthermore, modifications to the structure could involve a long process of cutting, shaping, and rewelding. To avoid the problems associated with employing the prototype (or parent) material as a modeling material, the use of another modeling material was pursued.

This report contains the results of research performed to understand the theoretical, analytical, and experimental methods necessary to determine if such an elastoplastic material can be either fabricated or obtained from currently available materials. The basic properties which this modeling material should possess include: (1) The nondimensional stress-strain curves (σ/E versus ε) for the model and prototype material should be the same; and (2) Poisson's ratio between model and prototype material should be the same. If a successful candidate material can be found, it would allow tests to be performed on a smaller, less expensive model and would permit testing of either the entire model or various sections under extreme loading to assess the ultimate strength or structural failure mode. Furthermore, modifications to the model could be made more expediently and at a lower cost than if a full-scale assembly were used.

The background section of this report presents a survey of past research into inelastic structural modeling. The second section will discuss the basic criteria which a model material must satisfy to extend modeling into the inelastic range. The third section presents an approach to satisfying these criteria. Finally, the experimental program undertaken to assess the validity of this approach is discussed.

BACKGROUND

A literature search was conducted to determine if any modeling technique exists which allowed the modeling of metallic structures in the inelastic range. Two facts soon became evident. First, the amount of research being done to physically model the inelastic behavior of structures is extremely limited; and, second, the work being done is mostly in the field of developing mathematical models of the cyclic-hysterisis loop of the material under consideration. For examples of this type of modeling, see References 6 through 9.

The literature search also revealed only two reports that discussed in detail physical inelastic modeling.[10,11] Numerous reports have been published on

small-scale model tests that have been performed assuming structural behavior stays within the elastic region. Among the materials used have been steel, aluminum, and other materials that are the same as the material used in the prototype. Rigid vinyl (polyvinyl chloride (PVC)), photoelastic materials, metal-filled epoxies, and various fiberglass composites are also commonly used modeling materials. Each of these has modeling advantages and disadvantages. The following sections address each material in more specific detail as it applies to elastoplastic modeling.

PHOTOELASTIC MATERIALS

The reports that have been written about the use of photoelastic methods to study the elastic response of structures are far too numerous to reference. Photoelastic materials have many of the same advantages as rigid vinyl in addition to the capability to cast various complicated parts and, by using three-dimensional stress freezing methods to determine stresses at an interior point of a structural member. Very limited literature is available on using photoelastic materials in the inelastic range.

Reference 10 is a report on using a photoelastic material as a method for inelastic stress analysis. The authors used three assumptions in developing the characteristics of their material: (1) the dimensionless stress-strain diagram for the model and prototype materials must be identical; (2) the yield strains for the model and prototype materials must be the same; (3) Poisson's ratio must be the same for the two materials. The approach taken by the authors was to form a mixture of rigid and flexible polyester resins.

The stress-strain curve of the resultant material could be varied significantly by changing the mixture ratios. One of the problems encountered was that of supply of the resins. At first, no manufacturer was willing to supply less than 45 gal of the resins at a reasonable price. This lack of supply caused a delay of six months before a supplier for a small quantity could be found. The conclusion reached in this search that "the polyester mixture is a suitable model material for many studies in the inelastic range of material response." Unfortunately, the authors chose only to say how good the model material was at duplicating an aluminum alloy (unknown) and did not provide a comparison of data. Because the model material characteristics did not lend themselves to modeling steel (in addition to the material availability problem), further pursuit of this method was abandoned.

METAL-FILLED EPOXIES

Two other possible candidate materials considered for use as an inelastic modeling material are an aluminum-filled epoxy and a lead-filled plastic.[11] Of these two materials only the lead-filled epoxy shows any promise. Aluminum-filled epoxies show little promise as a modeling agent for inelastic behavior for a number of reasons. Figure 1 shows a comparison of the nondimensional stress-strain curve for an aluminum-filled epoxy versus typical prototype materials. All data for the aluminum-filled epoxy were obtained from References 12 through 14. It can be quickly seen

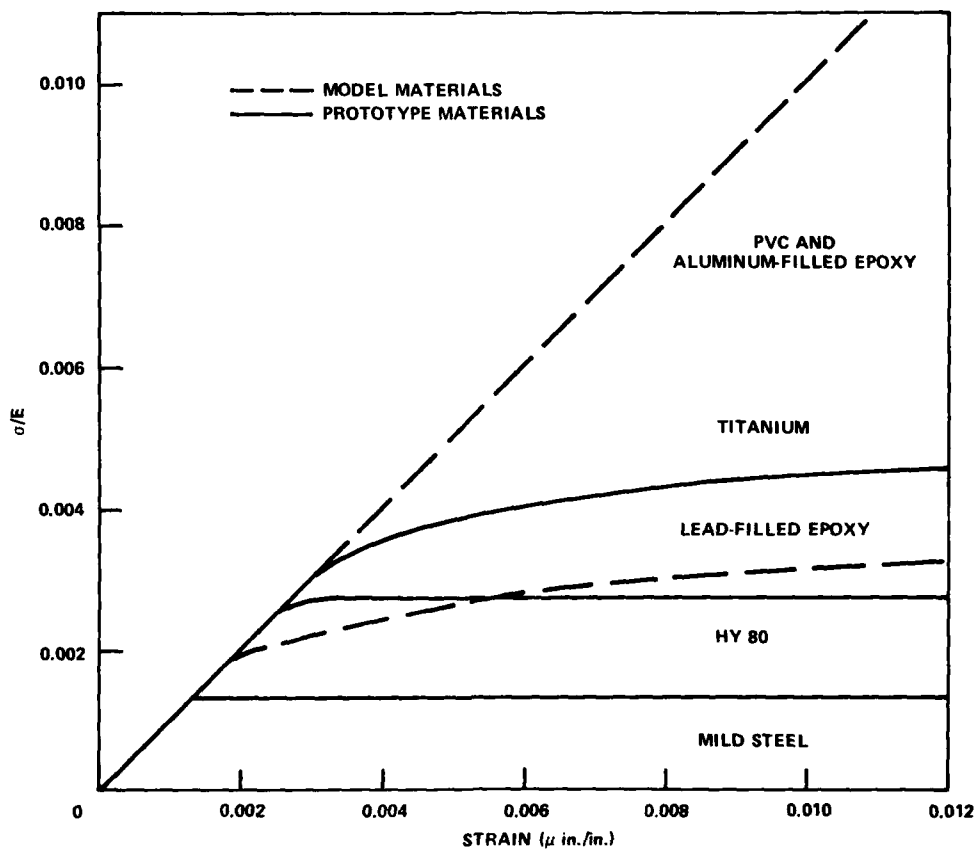

Figure 1 - Comparison of Model and Prototype Materials

that the yield and inelastic behavior in no way simulates that of steel. Another problem with the aluminum-filled epoxy (as well as with the lead-filled epoxy) is that it comes as a compound and needs to be mixed. This lends itself well for models that can be cast almost in entirety, but does not lend itself to models requiring a large number of various thickness of plates, as is commonly found on ship models.

An approach that has also been investigated is that of using a lead-filled epoxy as the modeling agent. This lead-filled epoxy consisted of a mixture of epoxy, plasticizer, and lead granules. The research determined what effect changing the ratio of lead to plasticizer and the ratio of lead to epoxy had on the stress-strain curve of the material. Figure 1 also gives a typical stress-strain curve of this material compared to prototype structural materials. One of the conclusions reached during this research was that, while giving a good representation of the elastic and inelastic response of high strength steels, the material did not accurately model the stress-strain response of the mild steels that are typically found on ships.

Certain manufacturing problems concerning this material should also be mentioned. In order to fabricate the lead-filled epoxy, it is necessary to mix the components in a container and then spray the contents onto a mold. The spraying allows a certain amount of the plasticizer to evaporate into the atmosphere, thus changing the character of the processed material. Because of the quality control problems associated with spray forming and the difficulties associated with spray forming this material into plate form, this approach was also not pursued further.

RIGID VINYL

For years, DTNSRDC and others have used rigid vinyl (PVC sheets) to construct structural models of ships, sections of ships, helicopter landing decks, various subassemblies of ships, automobiles, etc. Results and experimental procedures used in some of these tests are documented in References 15 and 16. Figure 1 also gives a typical stress-strain curve (nondimensional) for PVC compared to various materials. Scaling laws allow easy transformation from elastic strain on a PVC model to the elastic strain on the prototype. Once outside of the linear elastic portion of the corresponding prototype material, these scaling laws are invalid. Although PVC has superior model making characteristics (such as size and thickness availability);

thickness quality control; ease of cutting, shaping and joining; and low loads required to simulate prototype loads; it cannot be used alone as a modeling material for inelastic modeling.

FIBERGLASS-TYPE MATERIALS

The use of fiberglass-type materials was not pursued because of (1) fabrication problems for model size pieces and (2) response characteristics are sensitive to the direction of material lay up. (This effort is aimed at modeling isotropic materials.)

LITERATURE SEARCH SUMMARY

The search to find a modeling material or approach which is capable of reliably and econmically extending small-scale modeling into the inelastic range for the evaluation of metallic structural configurations commonly employed in naval vessels revealed no current material or method capable of achieving this goal. Table 1 presents an overview of currently employed modeling materials with their advantages and disadvantages. This lack of an established modeling method for reliably predicting structural inelastic response and ultimate strength led to the search for an alternative method which would achieve this goal. To accomplish this one must first examine the basic criteria which must be satisfied for a material to elastoplastically model another material.

BASIC CRITERIA FOR ELASTOPLASTIC MODELING

To elastoplastically model any structure, certain basic criteria must be met. The most important of these criteria deals with the stress-strain relationship between the model material and the prototype (or parent) material. Assuming classical structural scaling techniques[15,16] are employed, the stress-strain curves for parent and model materials can be nondimensionalized for comparison by plotting σ/E versus strain for both model and prototype materials. The strain at initiation of yield of both the model material and the parent material need not be the same. One can devise an additional scaling law to account for the difference in yield strains, if a model material of the desired material yield cannot be obtained. This will be

TABLE 1 - COMPARISON OF COMMONLY EMPLOYED MODELING MATERIALS

Model Material	Model Loads Required	Ease of Joining Small Pieces	Sheet Availability	Need to Manufacture in Lab	Load Direction Dependency	Shapability / Shaping Cost	Inelastic Response
Metal	Large	Difficult	Good	No	No	Difficult / Expensive	Yes
Rigid Vinyl	Small	Easy	Good	No	No	Easy / Inexpensive	No
Aluminum-Filled Epoxy	Small	Moderate	None	Yes	No	Moldable / Unknown	No
Lead-Filled Epoxy	Small	Unknown	None	Yes	No	Moldable / Unknown	Yes[2]
Photoelastic	Small	Easy	Good to Poor	Sometimes[1]	No	Easy / Inexpensive	Yes[3]
Fiberglass	Large	Difficult	Poor	Yes	Yes	Moderate / Expensive	Yes[4]

[1]Dependent on structure.
[2]Applicable mainly to castings.
[3]Aluminum only.
[4]If modeling fiberglass structures.

discussed in detail later. The ratio of the slopes of the elastic and plastic portions of the stress-strain curves should be identical. Finally, the model material should have the same Poisson's ratio as the parent material.

Another consideration is that the structural properties which are important to the particular model (such as the bending, axial, and torsional rigidities of the structure) be the same in the model and prototype. Finally, to ensure that the

failure mechanism of the model is the same as that for full-scale, the buckling behavior of the model must be the same as that for full-scale. That is, the structural model and full-scale structure should both become unstable (buckle) at the same scaled load levels either before or after the initiation of material yielding.

All of these basic criteria must be met to ensure that a structure modeled with a different material accurately predicts the elastic and inelastic behavior of the prototype structure being modeled. The next section demonstrates how a composite material approach can be used to meet these criteria and to elastoplastically model a metallic structure.

THEORY FOR COMPOSITE MATERIAL

The basic advantage sought in employing a composite material for structural modeling into the plastic range is reducing the ultimate size of the model (as well as the relative applied load) to obtain information about a structure's collapse mechanism and ultimate load. Since most interest and past research into the plastic behavior of structures centered on the use of mild steel, the main thrust of the development of an elastoplastic modeling technique was directed toward mild steel. To model the behavior of mild steel with a composite material, one would ideally want to develop a material with composite properties such that the model material yield strain is as near to the yield of the parent material as possible. An inequality of parent/model yield strains can, however, be overcome through the implementation of proper scaling laws, which will be addressed later. Additionally, the parent and composite materials should have the same slope ratios of elastic-to-inelastic modulus. Stated mathematically, these criteria are:

$$\varepsilon_{ym} = \varepsilon_{yp} \tag{1}$$

$$\begin{aligned} E_{em} &= E_{ep} \\ E_{pm} &= E_{pp} \end{aligned} \tag{2}$$

where ε_{ym}, ε_{yp} = yield strain of the model and parent material, respectively

E_{em}, E_{ep} = elastic modulus of model and parent material, respectively

E_{pm}, E_{pp} = plastic modulus of model and parent material, respectively (assumes bilinear behavior)

Elastoplastic modeling of a metal material behavior with a composite material can be achieved by reinforcing a less rigid matrix material with a stiffer material possessing the yield strain of the parent material. Visualizing the mechanism by which the reinforced composite material models a steel structure can best be accomplished by considering a simple tensile specimen made of a matrix reinforced with a certain percentage of reinforcement. Figure 2 shows two configurations in which the reinforcement can conceiveably be placed in the matrix. Figure 2a depicts a steel reinforcement distributed uniformly throughout the matrix. This type of reinforcement can be thought of as an infinite number of reinforcing strands uniformly arranged perpendicularly to the cross section such that the material behaves like a homogeneous material in that direction. Figure 2b depicts the steel reinforcement layered in two sheets between sheets of the less rigid matrix.

In each configuration, as the load T is applied to the tensile specimen, the force is resisted by both the matrix and the steel reinforcement; and the strains in both the matrix and reinforcement will be equal. In the elastic range the following force balance can be written

$$T = pA_T E_r \varepsilon + A_T(1-p)E_m \varepsilon \tag{3}$$

where T = applied tensile force

p = fraction of reinforcement by area (A_r/A_T)

A_r = area of reinforcement material

A_m = area of matrix material

A_T = total cross-sectional area

E_m = Young's modulus of matrix

E_r = Young's modulus of reinforcement

ε = resulting strain of composite material

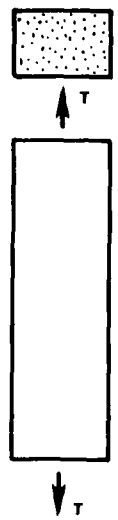

Figure 2a - Sprinkled Reinforcement

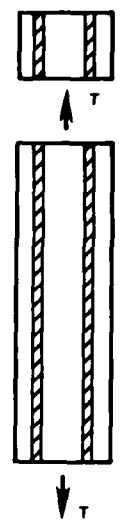

Figure 2b - Layered Reinforcement

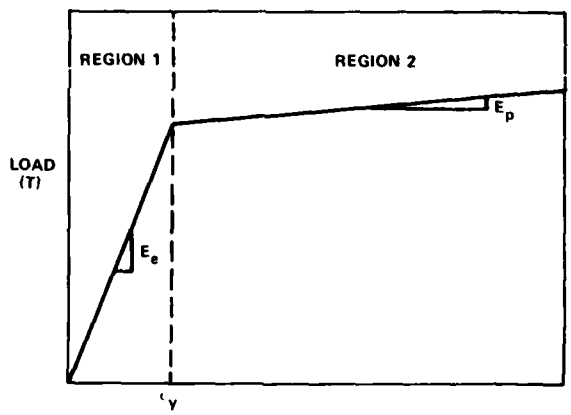

Figure 2c - Bilinear Load-Strain Relationship for Composites

Figure 2 - Concentrated and Uniformly Distributed Reinforcement Concepts and Load-Strain Behavior

Then, in the elastic range (before either the matrix or the reinforcement material has yielded) one can express the nominal elastic modulus of the composite material by dividing Equation (3) by A_T and the strain ε

$$E_e = E_N = \frac{T}{A_T \varepsilon} = \frac{\sigma_N}{\varepsilon} = pE_r + (1-p)E_m \tag{4}$$

where σ_N = nominal stress on composite cross section = T/A_T

$E_e = E_N$ = nominal composite elastic modulus = σ_N/ε

This portion of the composite stress-strain curve corresponds to Region 1 of the curve shown in Figure 2c with E_N corresponding to E_e in the same figure.

Now, to model the second portion of the material behavior (Region 2 in Figure 2c), one would ideally want to choose a matrix with a "material yield strain"* well above that for the parent material and a reinforcement material with the same "material yield strain" ε_{yr} as the parent material ε_{yp}, or

$$\varepsilon_{yr} = \varepsilon_{yp} \tag{5}$$

Then, when a sufficient load level was reached in the composite material to yield the reinforcement material, any additional load above this level would be resisted by the matrix material only when the plastic modulus of the reinforcement, E_{rp} is zero. We can now define the plastic modulus E_p for the composite material as the slope of the stress-strain curve after the reinforcing material has yielded. In this region (Region 2 in Figure 2c), only the matrix material will resist additional load ($E_{rp} = 0$) and the plastic modulus can be expressed from Equation (4) as

$$E_p = \frac{\Delta\sigma_N}{\Delta\varepsilon} = (1-p)E_m \tag{6}$$

The implication of using this approach is that the matrix modulus should be essentially constant in the strain region beyond the yield strain of the parent material being modeled and should remain elastic in this region if one wants to model a bilinear stress-strain curve. Additionally, one would want the ratio of E_p to E_e in Figure 2c to be similar in both the parent and model material (i.e., to

*"Material yield strain" is herein defined as the strain at the yield stress.

model steel, one would want $E_p << E_e$). We can express this ratio of the plastic-to-elastic modulus f in terms of the elastic moduli of the matrix E_m and reinforcement E_r and the fractional content by area of reinforcement material p. Doing this,

$$\frac{E_p}{E_e} = f = \frac{(1-p)E_m}{[pE_r+(1-p)E_m]} \tag{7}$$

By plotting E_r/E_m versus p for varying values of f (dependent on the parent material to be modeled), one can generate a family of design curves to arrive at the percent area of reinforcement material needed to model a particular parent material (i.e., to achieve the desired ratio of E_p to E_e). This was done to arrive at Figure 3.

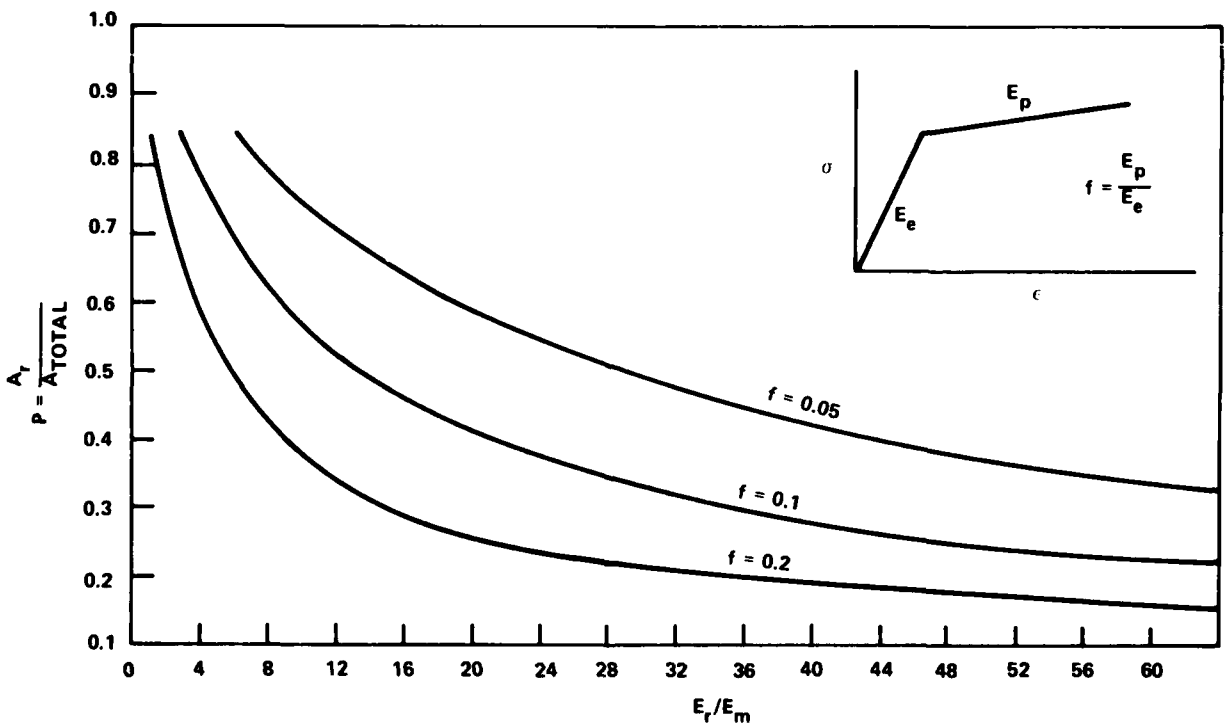

Figure 3 - Design Curves for Selecting Percent Area of Reinforcement Needed

For example, if one wanted to model steel, one would want an $f = E_p/E_e \leq 0.1$. Additionally, if the modeling materials were rigid vinyl ($E_m \approx 0.5 \times 10^6$) and steel ($E_r \approx 30 \times 10^6$) for the matrix and reinforcement respectively ($E_r/E_m = 60$), one would choose a reinforcement percentage ($p = A_r/A_T$) of at least 0.13 or greater.

Because of the complexity and cost of constructing a model material in the "sprinkled" manner of distributing the reinforcement as shown in Figure 2a, the sandwich method (layering the reinforcement material between the matrix material) was chosen. This layering of the reinforcement material poses the question of where in the cross section the reinforcement should be located to achieve the same bending moment to outer fiber strain relationship as in the uniform reinforcement case (the location of reinforcement for pure tensile behavior does not matter as long as the cross section possesses symmetry).

To achieve the proper plate bending properties for the reinforced material, one would want to locate the reinforcement such that, in both the elastic and plastic regions, the moment-surface strain (curvature) relationship is the same for the concentrated or 'sandwiched' reinforcement as it is for the uniformly distributed reinforcement. Then, for an arbitrary cross section in the elastic range, one would want

$$M_{UD} = \frac{E_{UD} I_{UD} \varepsilon_c}{c} = M_S = \frac{E_S I_S \varepsilon_c}{c} \tag{8}$$

where M_{UD}, M_S = moments of the uniformly distributed reinforcement and 'sandwiched' reinforcement cross sections for a strain ε_c at the section outer fiber

$E_{UD} = E_S = pE_r + (1-p)E_m$ = tensile elastic modulus of the composite model material

ε_c = strain on the cross section at a distance c from the neutral axis due to an applied bending moment

c = distance from neutral axis to extreme outer fiber of section

Because the two tensile moduli are equal for equal percentages of reinforcement by area p, then $E_{UD} = E_S$ and Equation (8) reduces to $I_{UD} = I_S$. Employing transformed section theory and the geometric properties for the rectangular sections shown in Figure 4a, one can approximate the inertial properties of each section (transformed

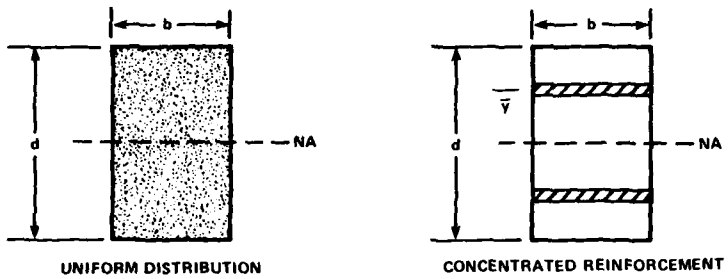

Figure 4a - Reinforcement Concepts

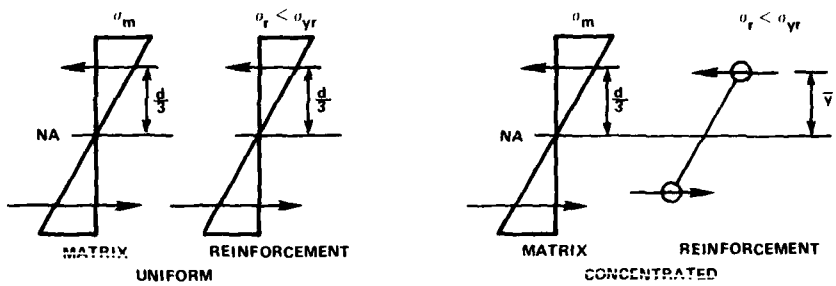

Figure 4b - Stress Distribution in Elastic Range ($\varepsilon < \varepsilon_{yr}$)

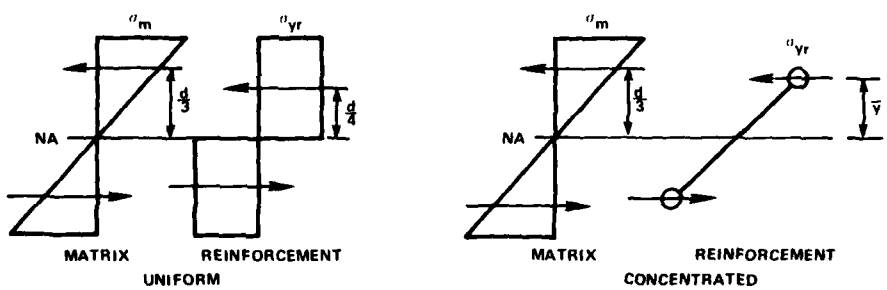

Figure 4c - Stress Distribution in Plastic Range ($\varepsilon > \varepsilon_{yr}$)

Figure 4 - Uniform and Concentrated Reinforcement Sections and Stress Distributions Across Cross Sections for Elastic and Plastic Cases

to matrix material only); and equating these, as in Equation (8), one can arrive at $\bar{y}$, the distance the reinforcement must be placed above and below the section's neutral axis to achieve the same elastic bending behavior in the sandwich reinforcement as in the uniform reinforcement.

$$\left[(1-p)\ \frac{bd^3}{12} + p\ \frac{bd^3}{12}\ \frac{E_r}{E_m}\right] = \left[(1-p)\ \frac{bd^3}{12} + pbd\bar{y}^2\ \frac{E_r}{E_m}\right]$$

$$\bar{y} = \frac{d}{\sqrt{12}} \tag{9}$$

Thus, the reinforcement should be located at $d/\sqrt{12}$ above and below the neutral axis to achieve the same elastic bending behavior in the sandwich reinforced and the uniform reinforced composites. To obtain the same bending behavior in the plastic range for the concentrated and uniform reinforcement, one can equate the bending moments on the cross section assuming that the section reinforcement has gone fully plastic, as illustrated in Figure 4c (i.e., all the reinforcement has yielded).

$$[M_{MATRIX} + M_{REINFORCEMENT}]_{UNIF.\ DIST} = [M_{MATRIX} + M_{REINFORCEMENT}]_{CONCENTRATED}$$

$$\left[\frac{E_m \varepsilon d/2}{2} \times \frac{1}{2}\ (1-p)bd \times \frac{2d}{3}\right] + \left[\frac{pbd}{2}\ \sigma_{yr}\ \frac{d}{2}\right] = \left[\frac{E_m \varepsilon d/2}{2} \times (1-p)bd \times \frac{2d}{3}\right] + \left[\frac{pbd}{2}\ \sigma_{yr}\ 2\bar{y}\right]$$

$$\bar{y} = \frac{d}{4} \tag{10}$$

Thus, the location indicated for the reinforcement in order to achieve the same bending behavior in the plastic range for the concentrated reinforcement and uniformly distributed reinforcement is at $\bar{y} = d/4$ above and below the neutral axis of the section. This result differs from the $\bar{y} = d/\sqrt{12}$ needed to achieve similar bending behavior in the elastic range. One can assess the effect of the concentrated reinforcement being positioned at these different locations by looking at the bending-strain relationship of an arbitrary section with the same tensile material properties. The section can be reinforced uniformly in one instance and reinforced with concentrated reinforcement at $\bar{y} = d/4$ and $\bar{y} = d/\sqrt{12}$ for comparison. This was done for the rectangular section shown in Figure 5 with the resulting moment-strain relationship also indicated in Figure 5.

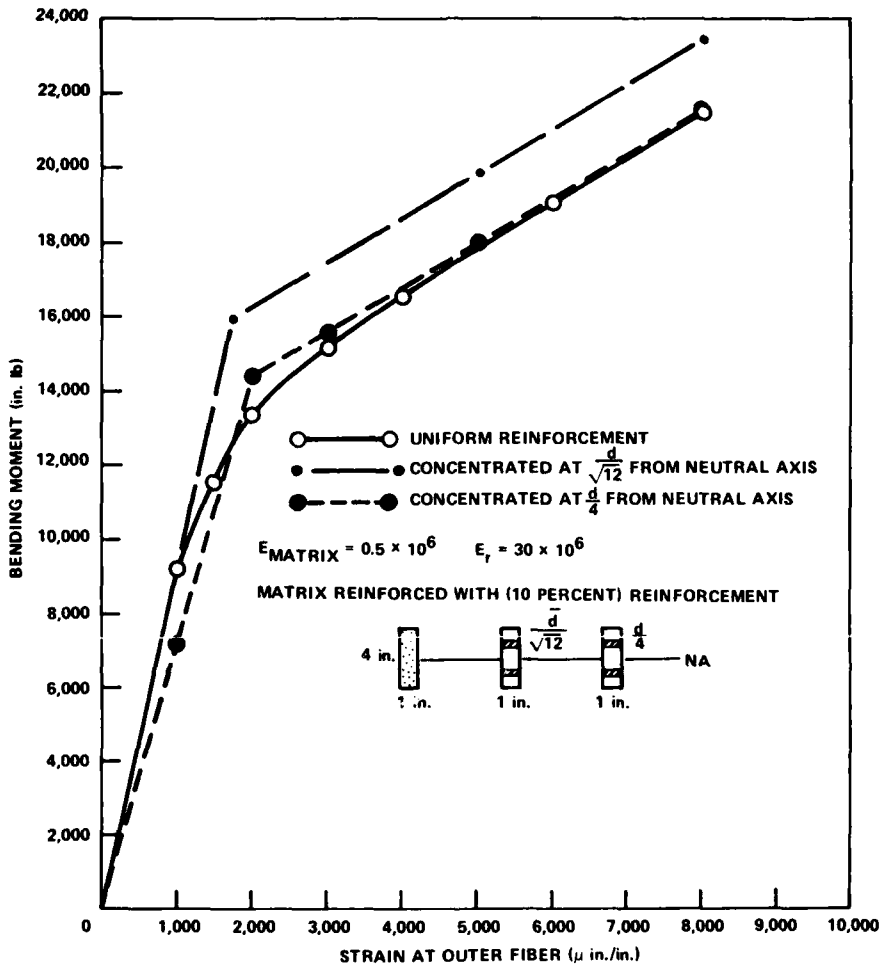

Figure 5 - Comparison of Reinforcement Location on Bending Behavior

One notes from Figure 5 that locating the concentrated reinforcement at $\bar{y} = d/4$ appears to provide the best overall representation of the elastoplastic bending behavior of the section, even though there is some deviation from the uniformly reinforced section in the elastic range. The main point to note from this figure is that one should use the reinforcement location (either $\bar{y} = d/4$ or $\bar{y} = d/\sqrt{12}$) that best suits the structural application desired. For example, one would want to employ the $\bar{y} = d/4$ reinforcement location in structural members where the expected mode of

failure would be the development of a plastic hinge from local bending moment; while the $\bar{y} = d/\sqrt{12}$ reinforcement location could be used for other members expected to encounter local strain levels below the elastic limit.

Another behavior mode which must be considered when selecting a reinforcement location for the concentrated type of reinforcement, is that of structural buckling. The procedure for determining the reinforcement location which accurately simulates this behavior is arrived at in the same manner as that employed for the case of bending moment behavior. That is, one can look at the engineering properties of which buckling is a function and equate the uniformly reinforced section to the concentrated reinforced section and solve for the location of the reinforcement. Then, with the concentrated reinforcement properly located, one can use conventional modeling theory to arrive at a properly scaled model. For elastic buckling, the Euler buckling load is[17]

$$P_E = \frac{\pi^2 EI}{L_e^2} \tag{11}$$

One would now want the uniformly reinforced and concentrated reinforced members to buckle at this same load. For a rectangular section

$$\frac{\pi^2 E_{UD}\left[(1-p)\frac{bd^3}{12}\frac{E_m}{E_{UD}} + \frac{pbd^3}{12}\frac{E_r}{E_{UD}}\right]}{L_e^2} = \frac{\pi^2 E_S\left[(1-p)\frac{bd^3}{12}\frac{E_m}{E_S} + pbd\bar{y}^2\frac{E_r}{E_S}\right]}{L_e^2}$$

and

$$\bar{y} = \frac{d}{\sqrt{12}} \tag{12}$$

which is the same result obtained for the elastic bending case.

The case of inelastic buckling presents no problem when using the reinforced composite material for modeling short column behavior. For this case, the critical buckling load can be arrived at by substituting the tangent modulus or E_t for E in Equation (12), as suggested by Engesser.[17]

$$P_{cr} = \frac{\pi^2 E_t I}{L_e^2} \tag{13}$$

This load is called the "Engesser load"[17] and accounts for different materials, inelastic effects, column length, column cross section, and end constraint. This equation indicates that the critical buckling load for a short column which would experience strains beyond the proportional limit of the material is simply a function of the tangent modulus of the material and no additional geometric properties other than were contained in the Euler buckling equation (Equation (11)). Then, for the case of the short column, one would want to locate the reinforcement in the cross section in the same location as for a long column ($\bar{y} = d/\sqrt{12}$). However, caution must be applied in analyzing any data where one expects short column behavior. The reason for this is that one must now be concerned not only with the bilinear stress-strain relationship between the model and prototype material, but also with the transition zone between the two linear portions of the stress-strain curves from where one is simulating pure elastic behavior to where one is simulating pure plastic behavior. This is the zone where the tangent modulus plays an important part in short column buckling. This fact can be readily seen in Figure 6, in which the slenderness ratio ($L/\sqrt{I/A}$) versus the critical buckling stress is plotted for a composite model material with the stress-strain relationship also indicated. That is, if one has a structural member with an actual slenderness ratio of $(L/\sqrt{I/A})_1 \leq (L/\sqrt{I/A})_{ACTUAL} \leq (L/\sqrt{I/A})_2$; then one must also try to assure that the tangent moduli in the transition zone between the elastic and plastic portions of the stress-strain curve are similar between the model and prototype material. This will ensure a reasonable degree of confidence in results obtained where buckling is expected in this region.

Thus, one can satisfy the basic criteria for using the concentrated reinforcement approach by locating the reinforcement to suit the application desired. For example, to model a ship hull girder in this way to determine the initiation of plasticity in the hull plating due to overall bending moment, one need not concern oneself with the location of the reinforcement with respect to the hull plating thickness (as long as the reinforcement is located symmetrically about the plating

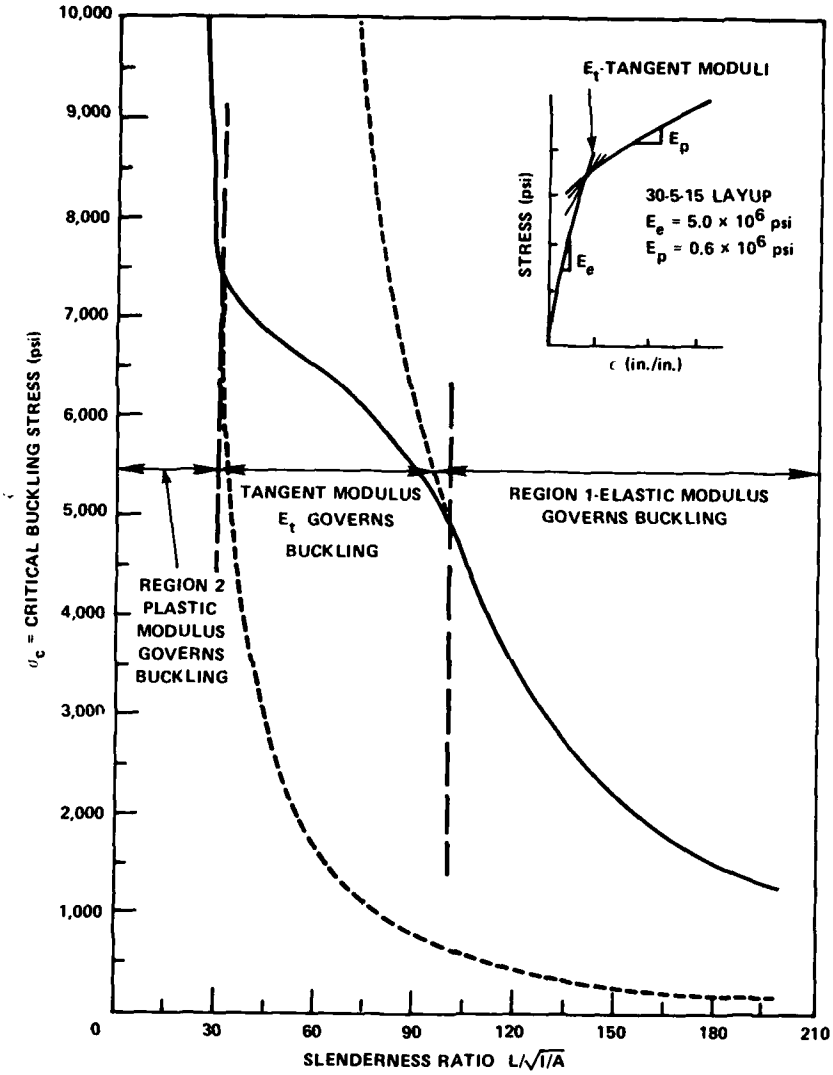

Figure 6 - Critical Buckling Stress versus Slenderness Ratio for a Composite Material

neutral axis). This is because the plating on the hull would be subjected to simple tensile and compressive strains (assuming no local elastic plate buckling occurred before the proportional limit was reached). If it is desired that local buckling effects be modeled in the particular hull girder panels, one would want to reinforce the plating at $d/\sqrt{12}$ from the neutral axis.

Another instance might be of interest in the local plastic bending behavior of a particular plating panel being loaded locally by a concentrated load. In this case, the reinforcement would be located at d/4 from the neutral axis to more accurately represent the plastic bending behavior of the panel.

Up to this point we have considered only the use of classical scaling techniques (reflecting the differences in material modulus and geometric scale ratio) to model the structure. If a reinforcement material is employed which has a yield strain which differs from the prototype, an additional scaling factor must be introduced to account for the difference in material behavior when analyzing the ultimate load capacity of the structure.

Using the classical scaling relationship of keeping strains in the model and prototype equal ($\varepsilon_m = \varepsilon_p$) and $\lambda L_m = L_p$ (where λ is the scaling factor), one can express the relationship between stresses in the model and prototype as

$$\varepsilon = \frac{\sigma_m}{E_m} = \frac{\sigma_p}{E_p} \text{ or } \sigma_p = e\sigma_m \tag{14}$$

and the relationship between model and prototype loads (or forces $\sigma = F/L^2$) as

$$F_p = e\lambda^2 F_m \tag{15}$$

Now, if one desires information as to the ultimate load of a structure where the model and prototype material possess different yield strains ($\varepsilon_{yp} \neq \varepsilon_{ym}$), one must employ an additional scaling factor on the model to determine the ultimate load of the prototype. The additional scaling factor is α where

$$\alpha = \frac{\varepsilon_{yp}}{\varepsilon_{ym}} \tag{16}$$

and the ultimate load for the prototype can be expressed as

$$F_{p_{ULT}} = F_{m_{ULT}} \, e\lambda^2\alpha \tag{17}$$

This scaling relationship would be employed where one desired information as to the ultimate loading a structure or substructure could attain. The instance may arise in which one is modeling a particular prototype material with a composite that has a reinforcement that possesses a yield strain higher than the prototype material. For this case, strains recorded beyond the prototype material yield point would not be accurate; but use of the scaling factor α would enable one to assess the ultimate strength of the prototype.

Changing scaled thicknesses for a specific purpose, as is done in rigid vinyl modeling,[15] can be done in certain instances in elastic-plastic modeling but one must pay particular attention to the consequences. For instance, if one were to smear the stiffeners into the hull plating to arrive at the same overall hull girder stiffness, one would be able to assess the overall strength of the hull girder if material yielding were the only criteria for failure. If a plating panel of the prototype hull girder were to have local buckling as a consequence of the overall hull girder loading and as part of the hull girder failure mode, one would want to assure the model behaved similarly. But the smearing of the stiffeners into the hull girder plating to achieve the same overall stiffness properties might change the local panel buckling behavior and thus give an erroneous result for the hull girder ultimate strength. This is because the scaling of this local buckling behavior would be a function of the panel's local geometric configuration and local buckling might not occur at the expected level if a distorted thickness is employed. Table 2 provides a list of scaling relationships for elastic-plastic modeling assuming there is no distortion of thickness.

EXPERIMENTAL VALIDATION

It was felt that the concept of a uniformly distributed reinforcement pattern, although more advantageous from the standpoint of providing a more accurate elastoplastic response for a section, would possess too many fabrication problems to be worked out within the time and budgetary allowances of this program. Further, the concentrated reinforcement material would be easier to fabricate and would still establish the validity of the composite approach for elastoplastic modeling of a structure.

TABLE 2 - TYPICAL SCALING RELATIONSHIPS FOR ELASTIC-PLASTIC MODELING

Fixed Quantities	
Length (Thickness)	$\lambda = L_p/L_m$
Strain	$\varepsilon_p = \varepsilon_m$
Material Modulus	$e = E_p/E_m$
Material Yield	$\alpha = \varepsilon_{yp}/\varepsilon_{ym}$
Poisson's Ratio	$\mu_p = \mu_m$
Dependent Quantities	
Stress	$\sigma_p = e\sigma_m$
Shear Stress	$\tau_p = e\tau_m$
Force	$F_p = e\lambda^2 F_m$
Moment	$M_p = e\lambda^3 M_m$
Moment of Inertia	$I_p = \lambda^4 I_m$
Section Modulus	$S_p = \lambda^3 S_m$
Axial Deformation	$\delta_p = \lambda\delta_m$
Ultimate Force	$F_{p_{ULT}} = F_{m_{ULT}} e\lambda^2\alpha$
Ultimate Moment	$M_{p_{ULT}} = M_{m_{ULT}} e\lambda^3\alpha$

Using the concentrated reinforcement approach, an experimental program was undertaken to (1) establish the tensile elastoplastic stress-strain behavior of the composite material using small tension specimens, (2) show the development of a plastic hinge in a simply support rectangular bending specimen, and (3) demonstrate the concept's validity for modeling elastic buckling in conjunction with determination of the ultimate strength of a total structure modeled using the composite

reinforcement approach. The structure chosen to model was a plate girder expected to fail in a web buckling mode. The plate girder chosen was a model of a mild steel plate girder tested by Rockey, et al.,[22] for which experimental data is available.

COMPOSITE MATERIALS

The basic criteria for selecting a reinforcement material was that the reinforcement material should have the same yield strain as the parent material (mild steel) and that the ratio of E_p/E_e be similar to that of the parent material (also dependent on matrix properties). Another criteria to consider was the availability of the reinforcement material in the desired thickness. For example, if one were to model a 1/8-in. plate using the concentrated reinforcement approach with a p = 1/10 and a scale ratio of 2, one would need a reinforcement thickness of 0.003 in. With all of the above criteria considered, a stainless steel reinforcement of 0.005 in. and a scale ratio of 1.893 was arrived at because of material yield, elastic modulus, and material availability considerations.

Rigid vinyl (PVC) was selected as the matrix material because of its low elastic modulus (0.5×10^6 psi) and because of its ability to stay elastic for large strain magnitudes beyond the yield of the reinforcement. Additionally, rigid vinyl is readily available in a wide variety of sheets from 0.010-in. to 0.125-in. thick, is easy to work, and is an established modeling material.

FABRICATION OF COMPOSITE PLATES

Prior to fabrication of laminates for use in the material testing program, a series of experiments was performed to determine which of several candidate adhesives would perform best for bonding rigid vinyl and stainless steel. Four epoxies were evaluated: HYSOL 0151 CLEAR, SHELL 815, AMICON XT-2526, and HYSOL EA 9309. Shear bond samples were fabricated and tested to failure. The shear strength of the HYSOL 0151 CLEAR, SHELL 815, and HYSOL EA 9309 were 508 psi, 258 psi, and 262 psi shear, respectively; and these three epoxies were eliminated. The AMICON XT-2526 samples all failed by fracture of the PVC material, leading to shear and bending loads on only one side of the sample (1/2 the shear area). The average failure load of 983 lb (1 sq in. total shear area) suggests that if the PVC material had not

fractured, the samples would exhibit a strength of at least 2000 psi. The composite samples and the plate girder model were fabricated using this adhesive, although its cure time was a full 7-day period.

Fabrication of the specimens for the various experiments described in this report was best accomplished by applying adhesive to each layer in the composite as it was assembled, and then pressing several samples (separated by wax paper) in a jig. The jig was constructed of two flat wood blocks, one with pegs around the perimeter of the sample shape, the other with matching holes. The jig allowed pressing of the samples (10 psi pressure) without sliding of the various components, and allowed many samples to be made at one time (this can be critical in view of the adhesive's 7-day cure time). The optimum glue thickness of 0.002 in. to 0.004 in. was attained using this method.

Of special note on the stainless steel used are the surface preparation requirements. All surfaces (including rigid vinyl) were "cross-hatch" sanded, and chemically cleaned to assure bonding. However, it was found that the steel required further treatment because of its manufacturing process. During the rolling of the thin stainless steel sheet the material becomes oil-impregnated and must be soaked at least overnight in trichloraethane or trichloroethylene. This caused no problems for the 1 in. × 14 in. samples, but the large plates fabricated for the plate girder model had to be soaked in a specially made tank.

The fabrication of the large plates for the plate girder model proved difficult. Applying and spreading adhesive to each layer, and pressing the pieces to remove the excess did not work as well as it had for the small samples. The large plates were pressed between flat wood boards to remove both air and adhesive. However, soft spots in the wood caused several bulges of adhesive between laminates. These were later shaved down with a plane. There were also voids where no adhesive had flowed. The outer layer of rigid vinyl was slit and adhesive was injected into the voids and repressed. In general, the glue thickness was not uniform throughout the plates. It is felt that the clamping pressure of 10 psi used for small samples was not attained for the plate girders due to the large areas involved and the fact that the pressure was applied simply by woodworking clamps. If future efforts are directed

toward this modeling technique, it would be wise to investigate mass production techniques for fabricating the required composite layups according to the designers' specifications to ensure better quality control.

TENSION TESTS

Two series of tension specimens were tested to establish the basic material properties of the composite material. The first series of tests sought to establish the tensile stress-strain behavior of the reinforcement material. To do this, 1-in. wide × 14-in. long strips of the stainless steel were cut and glued between gripping plates at either end. Strain gages were then applied and the specimens were subsequently pulled in tension. The resulting stress-strain diagram for a typical specimen is shown in Figure 7. The average modulus for the three stainless steel tensile specimens tested was found to be 31.5×10^6 psi, and the material was found to be fully yielded at an average of 45,000 psi. A typical rigid vinyl stress-strain curve is given in Figure 1.

The second series of tests defined the tensile stress-strain behavior of two layups of the composite material, one of which was used to fabricate the plate girder. The first layup (which was used for the girder) is shown in Figure 8 and consists of a 0.030-in. sheet of rigid vinyl sandwiched between two sheets of 0.005-in. stainless steel, which are in turn sandwiched between two sheets of 0.015-in. rigid vinyl; this layup will be referred to as 30-5-15. The tension specimens were fabricated in strips 1-in. long × 14-in. wide with an overall thickness of 0.072 in. The added thickness caused by the adhesive used to glue the layers together was not counted on from a strength standpoint. This fact was evidenced when tensile specimens with 0.005-in. glue lines were tested and the composite material exhibited the same strength as tensile specimens which had 0.002-in. glue lines (i.e., the same composite material modulus). The finite thicknesses mentioned above give the calculated quantities for the composite material properties shown in Table 3. Aluminum blocks, 1-in. square by 1/8-in. thick, were then glued to the tension specimens and holes were subsequently drilled through the blocks to accommodate the insertion of pins through which the tension loads were applied.

The necessary data were collected to demonstrate the materials bilinear stress-strain behavior. A typical stress-strain curve for the samples tested is shown in

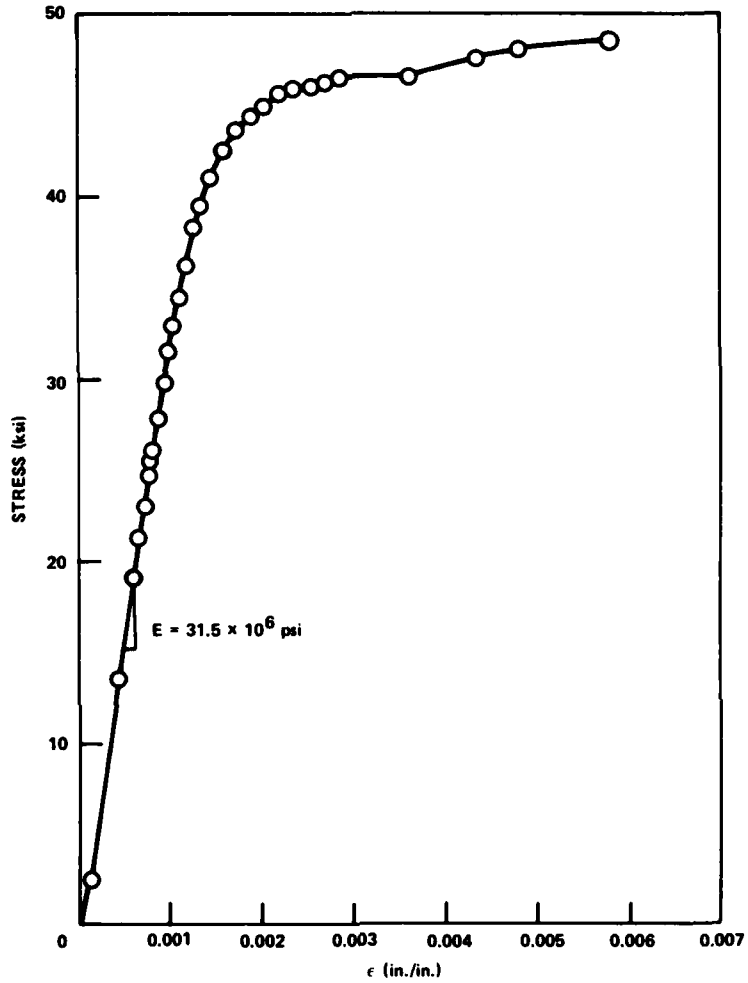

Figure 7 - Stress-Strain Characteristics of Steel Reinforcement

in Figure 8. Figure 8 also shows a hysteresis loop generated for this particular specimen which is a response similar to what one would obtain for an all metallic specimen. The average experimental properties for these tests are given in Table 3 for comparison with the calculated properties. One will note that the material behaves as predicted. Poisson's ratio was measured for the tension sample shown in Figure 8 and was found to be 0.29, which was anticipated since Poisson's ratio is approximately 0.30 for both rigid vinyl and steel.

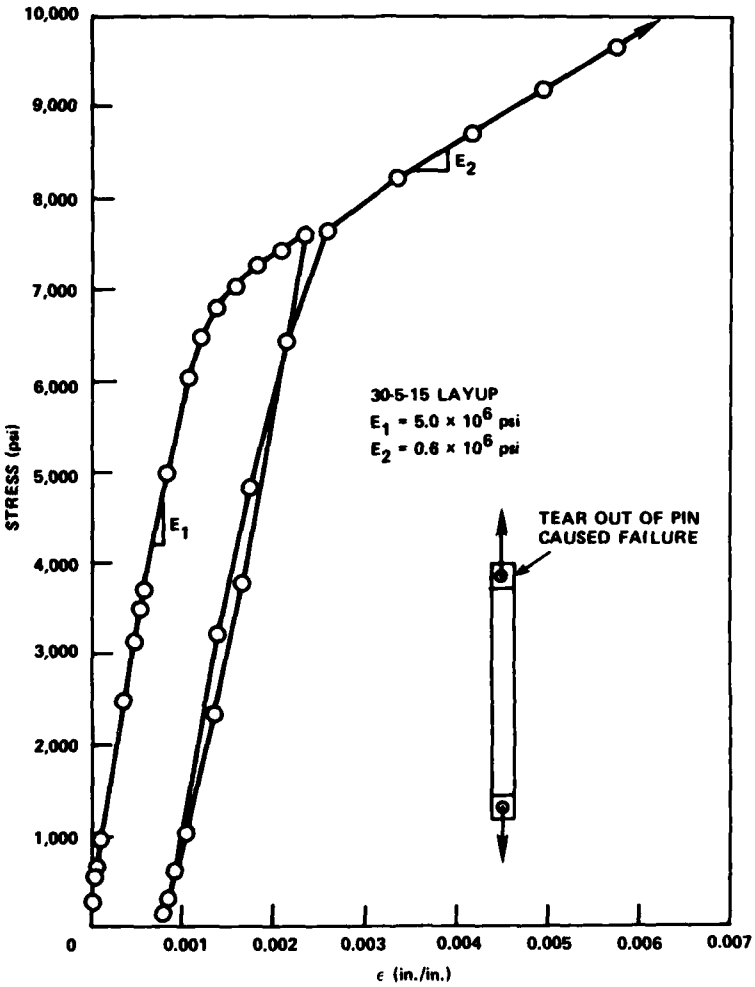

Figure 8 - Stress-Strain Characteristics of 30-5-15 Composite

The second layup examined was a 60-5-25 configuration, a 0.060-in. strip of rigid vinyl sandwiched between two 0.005-in. strips of steel which are in turn sandwiched between two 0.015-in. sheets of rigid vinyl. The tensile specimens were again made 1-in. wide by 14-in. long, with a nominal thickness of 0.12 in. The calculated material properties are also shown in Table 3, along with the average material properties from the experimental tensile specimens. A typical stress-strain curve for the 60-5-25 layup is shown in Figure 9. One will note the good correlation between experimental and predicted material properties from Table 3.

TABLE 3 - EXPERIMENTAL AND CALCULATED MATERIAL PROPERTIES FOR STEEL-REINFORCED RIGID VINYL COMPOSITE

Quantity	Layup			
	30-5-15 Calculated*	30-5-15 Experimental**	60-5-25 Calculated*	60-5-25 Experimental**
Elastic Modulus E_1 (psi)	5.19×10^6	5.07×10^6	3.08×10^6	3.05×10^6
Plastic Modulus E_2 (psi)	6.03×10^5	5.97×10^5	5.61×10^5	6.00×10^5

*The finite strength of the stainless steel was used in calculating the plastic modulus of the composite material since $E_{t(stainless)} \neq 0$ and Equation (6) becomes

$$E_2 = pE_{rp} + (1-p)E_m$$

where E_{rp} is the plastic modulus of the reinforcement.

**Average of all tensile specimens (3).

BENDING TESTS

Bending tests were conducted on both the 30-5-15 layup and the 60-5-25 layup. The bending specimens were fabricated not unlike the tensile specimens in that they were 1-in. wide by 14-in. long by the thickness of the respective layup. The specimens were then cut to an 8-in. length and had small pieces of rigid vinyl glued to them to keep them from sliding over the unrestrained knife edges used for simple supports. The pieces of rigid vinyl were glued to the bending specimens to achieve a simply supported span of 6 in. The specimens were then loaded with a two-point loading to achieve a pure bending moment at the center of the span where the tension and compression faces of the specimen were strain gaged. The test configuration is sketched in Figure 10a and a specimen undergoing plastic deformation is shown in Figure 10b. The two different layups of the composite bending specimens were used

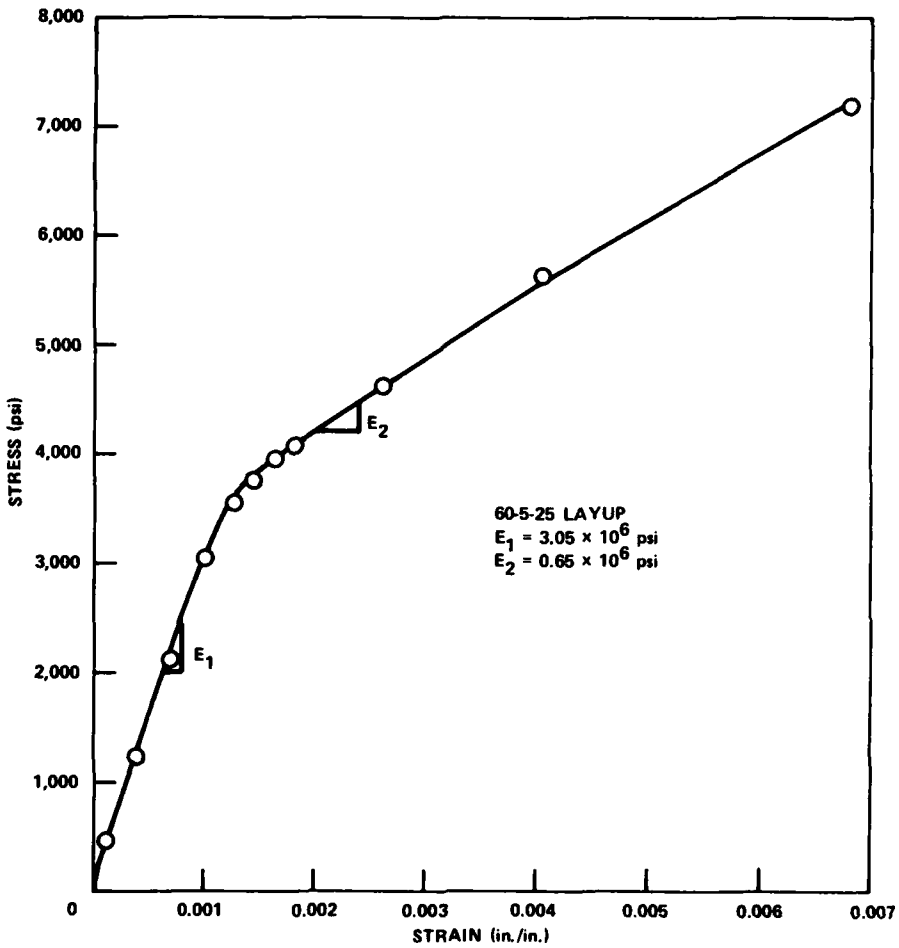

Figure 9 - Stress-Strain Characteristics of 60-5-25 Composite

to depict the difference in bending moment to outer fiber strain relationship between a beam with reinforcement located at d/4 from the neutral axis (30-5-15) and a beam with reinforcement located at approximately $d/\sqrt{12}$ from the neutral axis (60-5-25).

Figure 11 shows the experimental bending moment/outer fiber strain results for a typical 30-5-15 layup tested in the bending test setup. Also shown in the figure,

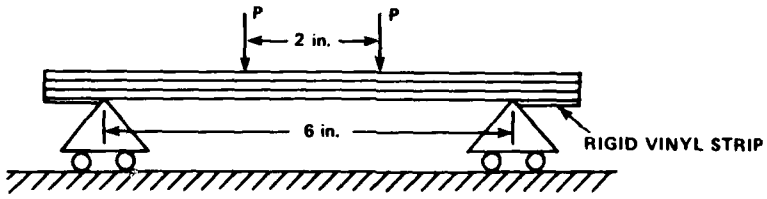

Figure 10a - Sketch of Bending Test Setup

Figure 10b - Bending Specimen Exhibiting Inelastic Deformation

Figure 10 - Bending Specimen Test Setup and Typical Specimen

in parenthesis, is a plot of the calculated bending moments needed to produce the same outer fiber strains in a solid steel beam with the same cross section. The all-steel section bending moments indicated in parenthesis correspond to the experimental model bending moments times the scaling factors $e\lambda^3$ (e.g., $M_{all\text{-}steel} = M_{composite}$

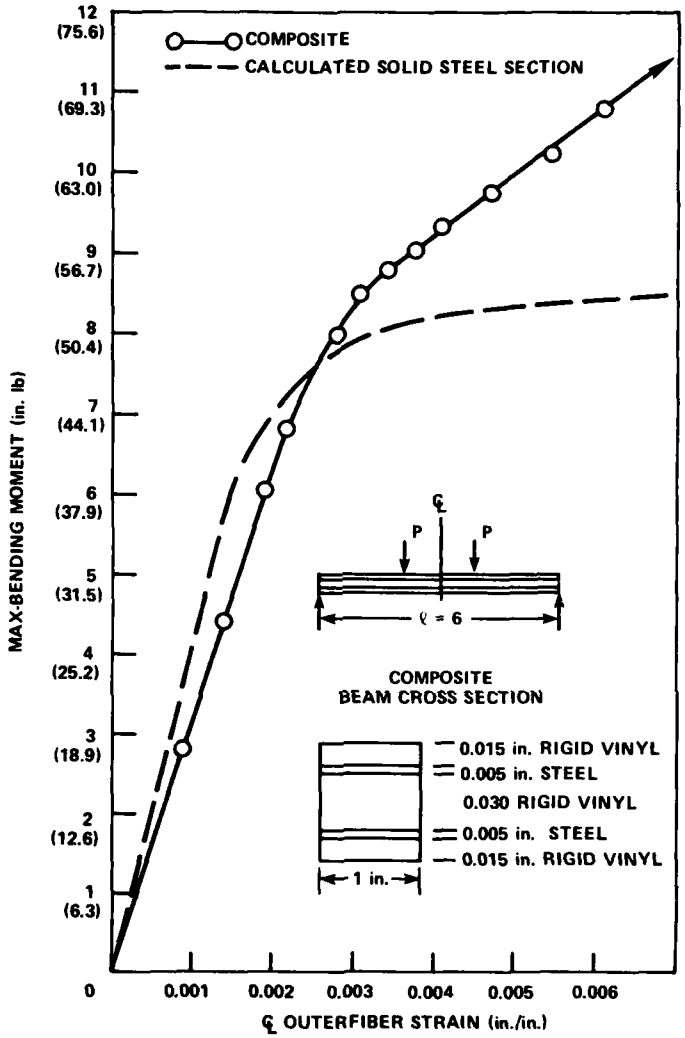

Figure 11 - 30-5-15 Composite Layup Bending Moment versus Outer Fiber Strain Characteristics

$e\lambda^3$; where $e = E_{steel}/E_{composite} = 31.5 \times 10^6/5.0 \times 10^6 = 6.3$ and $\lambda = L_{steel}/L_{composite} = 1.0$); thus making the two curves directly comparable. One will note from the figure that the knee in each curve occurs at relatively the same level of bending moment, and, as predicted, the composite model exhibits slightly less bending rigidity in the elastic range than the theoretical steel specimen does. The effect

where the plastic portion of the specimen moment-strain behavior overpredicts the ultimate moment capacity of the prototype can be rectified by increasing the percentage of steel (p) in the specimen. This would tend to decrease the slope of the second or plastic portion of the moment-strain curve. Another approach to reducing the plastic modulus E_p would be to employ a matrix material which has a modulus lower than rigid vinyl. The important point to be derived from these curves is that the knee of each curve occurs at the same moment level, which is the behavior the specimen was designed to exhibit, and that the total difference in strain energy between the two curves is not large. Additionally, the bending specimens exhibited the ability to withstand large amounts of strain (up to 20,000 micro strain) without any material failure or delaminations between the matrix and reinforcement material. This characteristic of the material demonstrates the composite's applicability for examining load conditions which would result in very high amounts of strain.

Figure 12 shows the bending moment to outer fiber strain relationship for the 60-5-25 layup (reinforcement at $d/\sqrt{12}$). Again, the theoretical relationship for a similar beam made of steel with a yield stress of 45,000 psi and an elastic modulus of 31.5×10^6 is also included in the figure. The bending moments for the solid steel beam which correspond to the model bending moments are indicated in parenthesis in the figure. One can see the exact correlation achieved between the composite bending specimen and the theoretical steel specimen in the elastic range. But, unlike the previous bending specimen with the reinforcement located at d/4 from the neutral axis, this specimen, as predicted in Figure 5, overpredicts the ultimate strength and the initiation of material yield that one would expect for a solid steel cross section. Thus, one should not employ this reinforcement layup (reinforcement at $d/\sqrt{12}$) in a situation where one desires to derive information as to the strength of a structure or substructure in an area where one wants to define the initiation of plastic behavior due to local bending.

BUCKLING TESTS

Separate buckling tests were not attempted due to the scope and time allowed for the project. Rather than pursue the validation of this behavior by designing and testing separate specimens, this aspect of the test program was not pursued because it was felt that the buckling of the web plating in the deep plate girder test would demonstrate the ability of the composite to model this particular structural behavior.

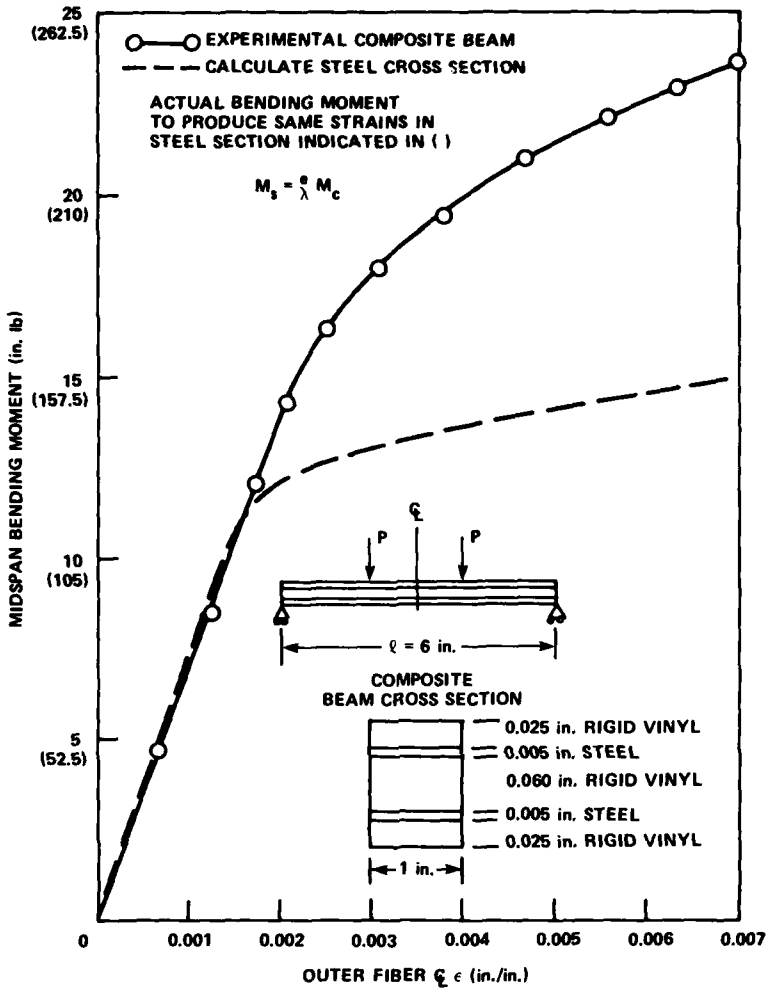

Figure 12 - 60-5-25 Composite Layup Bending Moment versus Outer Fiber Strain Characteristics

PLATE GIRDER ULTIMATE STRENGTH TESTS

Two model plate girders were fabricated using a $d/\sqrt{12}$ layup of the composite material. The plate girder is a scaled model of a plate girder tested by Rockey et al.,[18] to determine the ultimate load capacity of stiffened webs. The failure mode of the prototype girder was a buckling of the girder shear web and the development of a yielded diagonal tension field in the web. Additional loading of the

prototype girder produced a plastic hinge in the girder flange. The prototype girder was fabricated from 1/8-in. steel plate resulting in a scaling ratio of 1.893 ($\lambda = t_p/t_m = 0.125/0.066$). A sketch of the model girder is shown in Figure 13. The

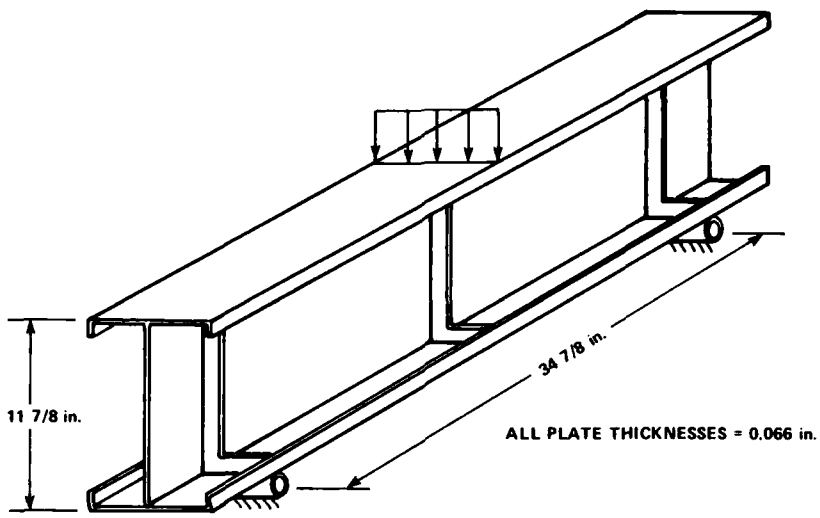

Figure 13 - Sketch of Composite Girder Configuration

prototype girder was fabricated from mild steel and had a material yield of 29.8 ksi and an ultimate collapse load of 59 kips. Since the yield strain of the prototype girder differs from that of the reinforcing material, the additional scaling factor α was employed to account for this difference in model and prototype material yield strains. Using the scaling relationships previously defined, one can calculate the expected ultimate load for the model girder to be

$$F_{m_{ULT}} = F_{p_{ULT}}/e\lambda^2\alpha = 59{,}000/(31.5/5.17)(1.893)^2(0.066) = 4057 \text{ lb}$$

The plate girder models were fabricated by first cutting the rigid vinyl and stainless steel pieces to the sizes needed to construct the component plates of the girder. Each of the component plates were made by gluing the rigid vinyl and steel

pieces together and applying pressure to the plate layup as described previously. Each component plate was then glued together to form the final girder configuration. To aid in developing the shear forces between the web and flange, small stainless steel angles (0.25 in. by 0.25 in. by 0.005-in. thick) were glued on each side of the web flange intersection. This step should not affect the results of the test, because the primary mode of failure is a buckling of the web panel and the development of a diagonally yielded tension field in the web panel. The plate girders were simply supported using rollers under the two outer web stiffeners and loaded across the flange over the center web stiffener.

Plate Girder 1 attained a load of 3400 lb when the center web stiffener began to trip causing a separation to occur between it and the web. The loss of the web stiffener caused the girder to fail in a web crippling mode under the point of load application. In this instance the glue line between the web stiffener and web proved insufficient to distribute the applied load to the web. The loss of the web stiffener left the web incapable of sustaining the local bearing load being applied, resulting in a local web crippling. Figure 14 shows the resulting failure mode, which is a classic deformation pattern for this type of failure. This premature failure of Girder 1 demonstrates the need to exercise extreme caution when designing and fabricating joints with this material as with any other modeling technique. That is, one must be sure that more than sufficient shear area is present when joining two members such that the shear forces can be transmitted without exceeding the shear strength of the glue line, unless this is the expected mode of failure. Additionally, one must be concerned with unwanted local instabilities of fittings.

To rectify this situation, 1/4-in. stainless steel angles (1/4 × 1/4 × 0.005) were glued to the web--web stiffener intersection on Girder 2 to develop more shear area than was available previously with only the thickness of the web stiffener providing the shear area. The manner of loading was the same as that for Girder 1. In this instance, the fix of providing more shear area between the web and web stiffener proved adequate and the girder developed the classic web buckling pattern with a diagonally yielded tension field. The web buckling can be seen in Figures 15a and 15b. Figure 16 illustrates the load versus midspan deflection characteristics of Girder 2. One will note that this curve resembles those curves for composite stress-strain or composite bending moment strain. The composite load deflection curve

Figure 14 - Web Crippling Failure of Composite Girder 1

continues to increase, as opposed to an all-steel structure which would resist taking more load, because of the strength still present in the rigid vinyl plate material after the steel reinforcement has yielded. For an all-steel girder, a yielded diagonal tension field develops in the web which resists no further load (i.e., the web material is more ideally elastic-plastic).

The composite girder model exhibited the same failure mode as the all-steel girder. This is evidenced by the web buckling that can be seen in Figure 15 and the formation of the yielded diagonal tension field which can be seen in Figure 17 (the strain levels in the girder web are beyond reinforcement yield). Also shown in Figure 17 is the growth pattern of the membrane strain versus applied load for a

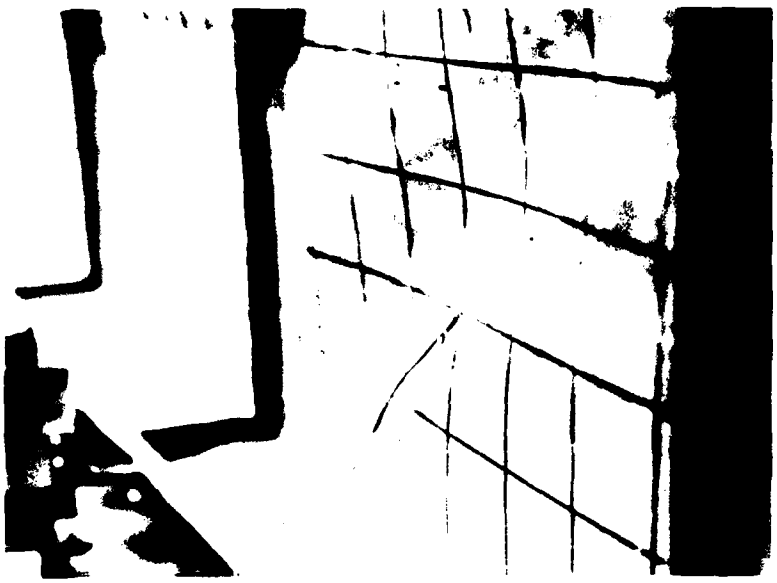

Figure 15a - Web Buckling at Ultimate Load

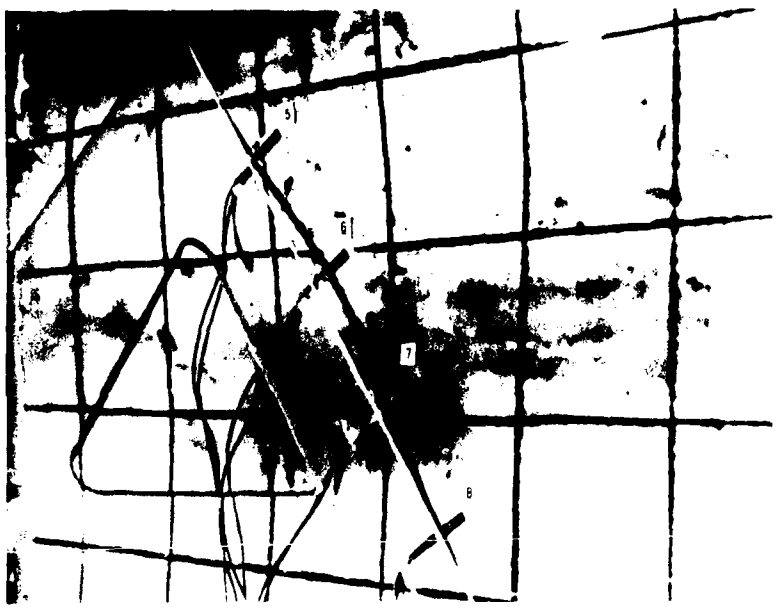

Figure 15b - Residual Deformation After Releasing Load

Figure 15 - Web Buckling of Composite Girder 2

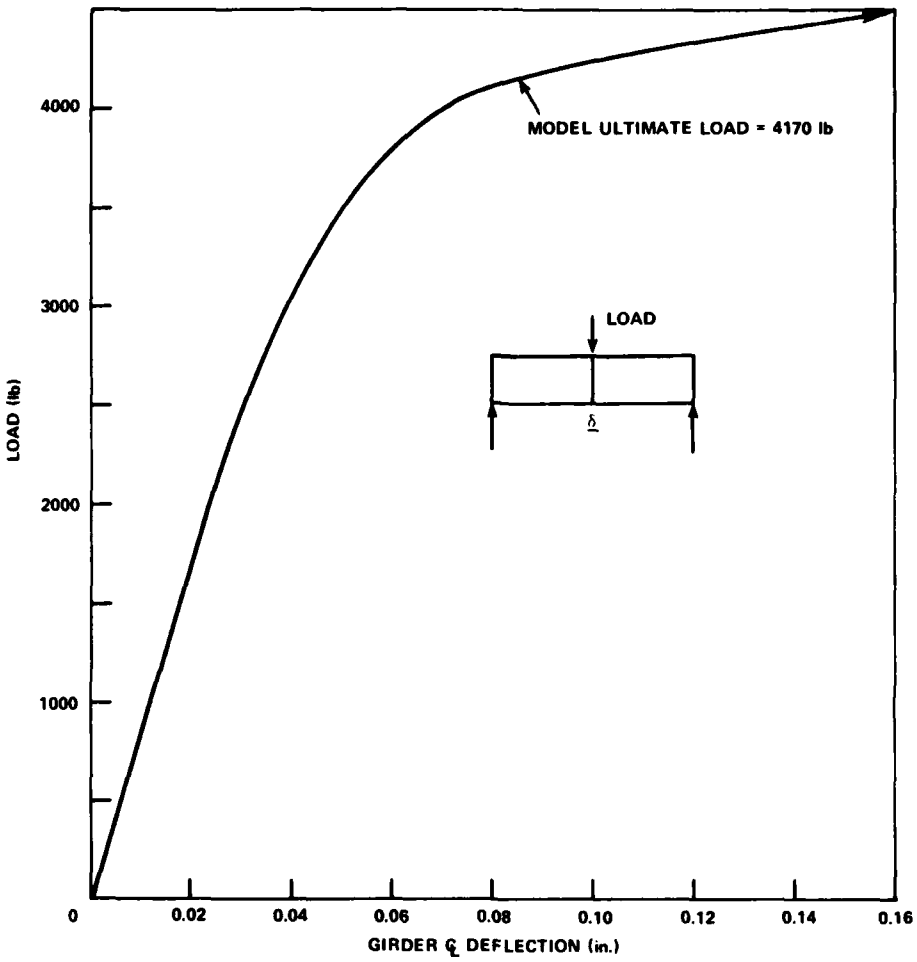

Figure 16 - Load versus Midspan Deflection for Girder 2

typical strain gage location. One will note the similarity in shape between this curve and the load deflection curve shown in Figure 16, indicating that it is material yielding and not joint slippage causing the observed load-deflection relationship.

The loading of the girder was terminated when it became apparent that large amounts of deflection were occurring for small increments of increasing load. The problem then becomes one of defining what the ultimate load of the structure is

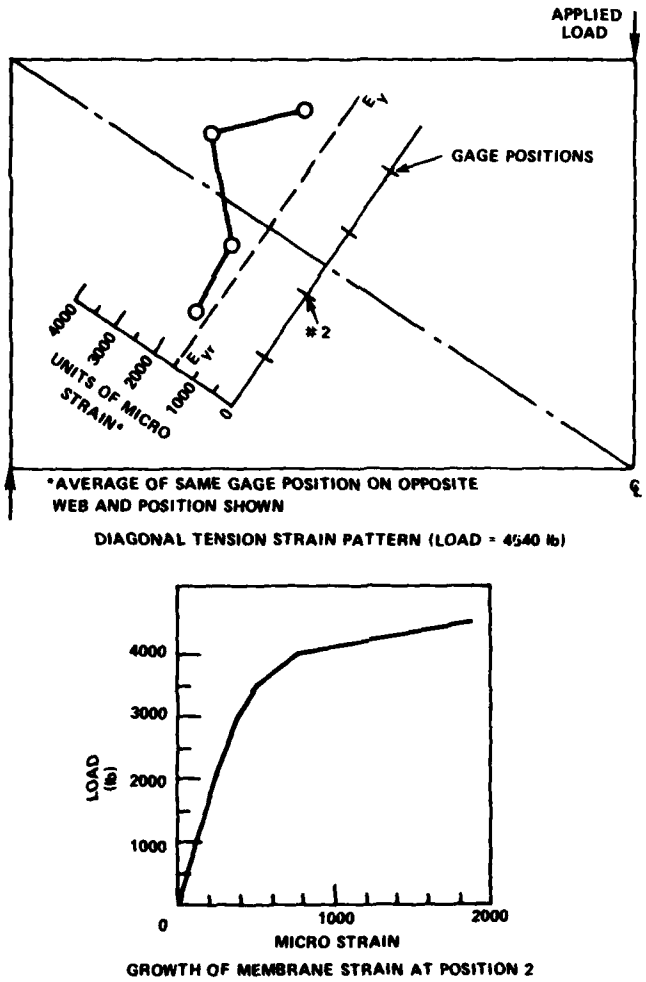

Figure 17 - Diagonal Tension Strain Patterns and Growth of Membrane Strain with Load

since the girder will continue to take load as it is applied. The reason the girder continues to have a positive sloped load-deflection relationship beyond the yield point of the reinforcement is due to the finite load carrying capacity remaining in the rigid vinyl (albeit much less than that of the composite as a whole). Then, a fair estimate of the ultimate load capacity of the composite model can be made by determining when the load-deflection curve of the girder attains a second linear

slope, which would indicate that additional load is being resisted only by the rigid vinyl. (This can be thought of as E_p on the stress-strain diagram.) This was done as is indicated on Figure 16, indicating an ultimate load of 4170 lb. This compares rather well with the previously calculated scaled value of 4057 lb.

Thus, one can see that having some knowledge of the anticipated failure mechanism is helpful for the successful implementation of this modeling technique and the interpretation of test results. In interpreting results one must look at the model failure mechanism and be aware of the relationship between the model composite material behavior and that of the prototype material behavior. These two parameters should be considered together when interpreting results and planning model evaluations.

SUMMARY AND CONCLUSIONS

Engineering analyses were developed for employing a composite material approach to elastoplastically modeling a structure. A test program, consisting of small tensile and bending specimens and a modeled structure, was conducted to validate the engineering analyses. The test program established that the proposed method was indeed a viable way of extending modeling techniques into the inelastic range.

A deep plate girder structure was modeled for which the inelastic behavior was known and for which data is available pertaining to collapse load and deformation pattern. The model developed the predicted failure mechanism, a classic web buckling with a fully developed diagonal tension field, and attained an ultimate load which agreed well with the scaled-prototype, experimentally obtained ultimate load. This demonstrated the potential of this approach to structurally extending small model testing into the inelastic range. The method has the capability of being able to determine the relative ultimate load of a structure and would probably find its best implementation as a tool by which one could compare the relative ultimate strengths of different structural configurations. However, care must be exercised in that, if the relative strength of structural members in tension, bending, and buckling and their contribution toward the collapse mechanism are not known, erroneous results may be obtained.

All of the investigations on the current effort were aimed at simulating the structural behavior of steel structures. This was done because of reinforcement

material availability and because of the large concentration of past investigations on full-scale steel structures into the inelastic range. Because of the nature of the bilinear stress-strain curve of the composite modeling material, a more accurate representation of an aluminum material could be made because of the similarity of the aluminum stress-strain curve. Comparison of the stainless steel-PVC composite stress-strain behavior with that of aluminum indicates that this particular model material composition would apply well to modeling aluminum structures. The problem with modeling steel using this approach is that to make the plastic modulus much smaller than the elastic modulus ($E_p << E_e$), one must increase p (which in turn increases Young's Modulus, model loads, and weight) which tends to make the model resemble an all-steel structure, and the advantages of the composite approach become less pronounced. It appears that the most promising approach to elastoplastically modeling steel would be to employ a matrix material which has a modulus which is less than rigid vinyl, but still possesses a linear stress-strain relationship for very high strain levels.

An area which should be afforded much detail when using the composite approach, whether modeling aluminum or steel, is that of the fabrication of structural joints in the model. Because of the large strain levels associated with taking a structural model into the plastic range, one must pay particular attention to areas where components are attached, especially in areas of high shear stress. To assure that shear stresses are transferred from one member to another, one must supply an adequate shear area such that the shear stress at the bonded joint does not exceed the ultimate shear transfer capability of the bonding agent being employed.

Most importantly, to make this method more effective, a means of being able to economically produce sheets of the designed composite must be developed. The current method of cutting the pieces to the desired size and then laminating by applying pressure, should be replaced by an assembly which produces large sheets of the composite from which the desired size pieces could be cut.

An aspect not investigated is the ability of this composite approach to lend itself to the heat forming operations that are employed to develop a ship hull shape with rigid vinyl models or the molding type operations employed for fiberglass models. The method of heat forming and bending the composite does not appear

feasible, because one would likely initiate inelastic behavior in the molding process. This indicates one would have to find an alternative method of modeling the ships hull in area of compound curvature. Although the method as developed herein has much room for improvement, direct application in many cases of ultimate strength assessment is possible.

ACKNOWLEDGMENTS

The authors wish to express their appreciation to the following individuals whose support contributed to the meeting of the overall objective of developing a method of extending small-scale modeling into the inelastic range:

Messrs. William Hay and Fred Palmer of the Structures Department for assembling and operating the data acquisition system for the conduct of the deep girder ultimate strength evaluations.

Mr. Roger Milihram of the Industrial and Facilities Shops Department for his invaluable craftsmanship in the fabricating of the composite deep plate girder structure and the many smaller composite samples used in this project.

Dr. Milton Critchfield of the Structures Department who provided valuable guidance and suggestions in arriving at a suitable structure (a deep plate girder) which had been previously subjected to ultimate strength evaluations, and for which ultimate strength data exists.

REFERENCES

1. Bathe, Klaus-Jurgen, "Elastic-Plastic Large Deformation Static and Dynamic Analysis," Computers and Structures, Vol. 6, No. 2 (Apr 1976), pp 81-92.

2. McIvor, I.K. and H.C. Wang, "Plastic Collapse of General Frames," International Journal of Solids and Structures, Vol. 13, No. 3 (1977), pp 197-210.

3. Plaut, Raymond, "Post-Buckling Analysis of Non-Conservative Elastic Systems," Journal of Structural Mechanics, Vol. 4, No. 4 (1976), pp 395-416.

4. Wagner, A.L. and W.H. Mueller, "Ultimate Strength of Tubular Beam-Column," American Society of Civil Engineers, Journal of Structural Division, Vol. 103, No. 1 (Jan 1977).

5. William, J.G. and M. Stein, "Buckling Behavior of Structural Stiffeners of Open Sectioned Stiffened Composite Compressive Plates," AIAA Journal, Vol. 14, No. 11 (Nov 1976), pp 1618-1626.

6. Jones, Robert M., "NonLinear Multiaxial Modeling of Graphitic and Carbon-Carbon Materials," Air Force Materials Laboratory Report AFML-TR-76-215, Southern Methodist University, Dallas, Texas (Dec 1976).

7. Jhansale, H.R., "A Unified Approach For Modeling Inelastic Behavior of Structural Metals Under Complex Cyclic Loadings," Construction Engineering Research Laboratory Technical Report M-214 (May 1977).

8. Raghaua, R. et al., "The Macroscopic Yield Behavior of Polymers," Journal of Materials Science, Vol. 8 (1973), pp 225-232.

9. Iwan, W.D., "On a Class of Models for the Yielding Behavior of Continuous and Composite Systems," Journal of Applied Mechanics (Sep 1967), p 612.

10. Zachany, Loren W. and William F. Riley, "Photomechanics Methods for Inelastic Stress Analysis," U.S. Army Research Office Report DAHC-04-74-G-0105, Engineering Research Institute, Iowa State University, Ames, Iowa (Mar 1976).

11. Dalzell, J.F. and P.S. Westine, "A Study of the Feasibility of Dissimilar Material Modeling Techniques as Applied to the Response of Ship Structures to Water Impact," Southwest Research Institute Project No. 02-1767 (July 1966).

12. "Model Tech Applications Manual," Photoelastic, Inc., Bulletin MT-012.

PRECEDING PAGE BLANK-NOT FILMED

13. Riegner, E.I. and A.E. Scotese, "Use of Reinforced Epoxy Models to Design and Analyze Aircraft Structures," AIAA Journal of Aircraft, Vol. 8, No. 10 (Oct 1971), pp 813-817.

14. Scotese, A.E. and W.E. Nickola, "Advancements in Modeling and Testing Techniques for Aluminum Filled Epoxies," presented at 1975 Society for Experimental Stress Analysis Spring Meeting, Chicago, Illinois (May 1975).

15. Austin, S.L., "Design History of the Rigid Vinyl Model of the Hydrofoil Plainview (AGEH-1)," NSRDC Report 3883 (Oct 1972).

16. Rodd, J.L., "Verification of the Rigid Vinyl Modeling Techniques: The SL-7 Structure," Ship Structure Committee Report SSL-259 (1976).

17. Shanley, R.F., "Strength of Materials," McGraw Hill (1957).

18. Rockey, K.C. et al., "Ultimate Load Capacity of Stiffened Webs Subjected to Shear and Bending," Conference on Steel Box Girders (1973).

INITIAL DISTRIBUTION

Copies	
1	DDR&E Lib
1	CNO OP 098T
1	CHONR Code 474
1	DNL
2	CHNAVMAT 1 MAT 08T23 1 Lib
2	NRL 1 Code 8431 1 Tech Lib
1	USNA
1	NAVPGSCOL
1	NWC
1	NADC
1	NOSC Code 6342
14	NAVSEA 1 SEA 03 1 SEA 03C 1 SEA 03D 1 SEA 03R (Bennen) 1 SEA 03R (Pohler) 1 SEA 06D 1 SEA 312 (Kerr) 1 SEA 32 1 SEA 323 1 SEA 3231 (O'Brien) 1 SEA 3232 (Swann) 1 SEA 3233 (Gagorik) 1 SEA 62R 1 SEA 996
12	DTIC

Copies	
1	Wright-Patterson AFT AFFDL-FBEC
1	NSF/Engr Div Lib
1	Library of Congress
1	Secretary Ship Structure Committee U.S. Coast Guard Headquarters Washington, D.C.

CENTER DISTRIBUTION

Copies	Code	Name
1	012	
1	11	
1	112	
1	115	
1	117	
1	118	
1	15	
1	16	
1	17	
1	1702	
1	1706 (m)	
1	1720	
15	1730	
1	1740	
1	1750	
1	1770	
1	1770.7 (m)	
1	1844	
1	19	

Copies	Code	Name
10	5211.1	Reports Distribution
1	522.1	Unclassified Lib (C)
1	522.2	Unclassified Lib (A)

FILM

0-